

Nonlinear Precoding in the RIS-Aided MIMO Broadcast Channel

Dominik Semmler, Michael Joham, and Wolfgang Utschick

School of Computation, Information and Technology, Technical University of Munich, 80333 Munich, Germany
email: {dominik.semmler,joham,utschick}@tum.de

Abstract—We propose to use Tomlinson-Harashima Precoding (THP) for the reconfigurable intelligent surface (RIS)-aided multiple-input multiple-output (MIMO) broadcast channel where we assume a line of sight (LOS) connection between the base station (BS) and the RIS. In this scenario, nonlinear precoding, like THP or dirty paper coding (DPC), has certain advantages compared to linear precoding as it is more robust in case the BS-RIS channel is not orthogonal to the direct channel. Additionally, THP and DPC allow a simple phase shift optimization which is in strong contrast to linear precoding for which the solution is quite intricate. Besides being difficult to optimize, it can be shown that linear precoding has fundamental limitations for statistical and random phase shifts which do not hold for nonlinear precoding. Moreover, we show that the advantages of THP/DPC are especially pronounced for discrete phase shifts.

Index Terms—THP, LOS, DPC, vector perturbation, lattice

I. INTRODUCTION

RISs are viewed as a key technology for future communications systems (see [1]). These surfaces consist of many passive elements which allow to reconfigure the channel resulting in an improved system performance. While this technology gives new degrees of freedom for system optimization, the high number of reflecting elements also drastically increase the complexity. The channel estimation as well as the joint optimization of the precoders and the reflecting elements in a downlink scenario pose two major challenges for the technology. We consider perfect channel state information (CSI) in this article and the main focus will be on the second point, where we give a new algorithm for the joint optimization of the precoders and the reflecting elements in order to maximize the sum spectral efficiency (SE). For sum SE maximization under perfect CSI, there is already significant literature available, see, e.g., [2], [3], [4]. Additionally, we assume that the BS-RIS channel is dominated by a LOS channel which is motivated by the fact that both the BS and the RIS are both deployed in considerable height and in LOS conditions by purpose (see [5]). This assumption has already been considered in the literature (see, e.g. [6], [7], [8]).

Recently, it has been shown in [9] that especially nonlinear precoding techniques such as, e.g., DPC, are particularly suited for such a scenario. Following [9], it has been pointed out that it is crucial for the performance of the system that the BS-RIS channel is orthogonal to the direct channels. This condition is not met in a practical scenario and DPC is considerably more robust in comparison to linear precoding if this condition is not completely fulfilled. Furthermore, linear precoding suffers from fundamental limitations when considering random or statistical phase shifts (see [9]). As an example, in a rank improvement scenario under Rayleigh fading, the SE of linear precoding for random phase shifts is upper bounded by a constant whereas for DPC it is increasing monotonically with the number of reflecting elements. Because of the above mentioned benefits of DPC, we propose an efficient algorithm in this article based on THP (see [10], [11]). THP is a vector perturbation technique (see [12]) with reduced complexity which we show to share the same

benefits as DPC. There exist fundamental advantages over linear precoding that are especially pronounced for random or statistical phase shifts. We focus on random phase shifts and instantaneous phase shifts in this article, whereas statistical phase shifts will be analyzed in future work. Particularly, for discrete phase shifts, we observe that also for instantaneous phase shifts, THP has a significant advantage. In comparison to DPC, THP is simple to implement. However, it also comes with a certain performance loss. Specifically, it suffers from a shaping loss and we analyze its performance within this article. Our contributions are:

- We derive the high-signal to noise ratio (SNR) optimal solution for DPC in case where there are more users than base station antennas. Additionally, a low-complexity phase shift optimization for DPC is derived which can be shown to be optimal for specific scenarios.
- We propose THP for the RIS-aided scenario and give a low-complexity algorithm based on that method. In particular, we use distributed THP (dTHP) which appears to be better suited in comparison to centralized THP (cTHP) in a RIS-aided scenario.
- We compare DPC, linear precoding, and THP (including the shaping loss) in this article and show that THP has the same benefits as DPC shown in [9], specifically, we show discrete phase shifts to be an interesting aspect in favor of THP/DPC.

It has to be noted that throughout the article, we consider the conventional phase shift model which is the most popular model in the literature. However, a more accurate model has been given in [13]. The algorithms and results in this article can be directly extended to the model in [13] and, additionally, to mutual coupling by considering decoupling networks (see [14]).

II. SYSTEM MODEL

A scenario with one BS serving K single-antenna users is considered. The system is supported by one RIS with N_R reflecting elements. Furthermore, we assume the BS-RIS channel to be rank-one, i.e., $\mathbf{H}_s = \mathbf{a}\mathbf{b}^H$, where w.l.o.g. we assume $\|\mathbf{b}\|_2 = 1$. Hence, the channel of user k reads as

$$\mathbf{h}_k^H = \mathbf{h}_{d,k}^H + \mathbf{h}_{r,k}^H \Theta \mathbf{a} \mathbf{b}^H \in \mathbb{C}^{1 \times N_B} \quad (1)$$

with $\mathbf{h}_{d,k}^H \in \mathbb{C}^{1 \times N_B}$ being the direct channel from the BS to the k -th user, $\mathbf{h}_{r,k}^H \in \mathbb{C}^{1 \times N_R}$ being the reflecting channel from the RIS to user k , and $\Theta = \text{diag}(\boldsymbol{\theta}) \in \mathbb{C}^{N_R \times N_R}$ with $\boldsymbol{\theta} \in \{\mathbf{z} \in \mathbb{C}^{N_R} : |z_n| = 1, \forall n\}$ being the phase manipulation at the RIS. By defining $\mathbf{h}_{c,k}^H = \mathbf{h}_{r,k}^H \text{diag}(\mathbf{a})$ we arrive at the equivalent expression

$$\mathbf{h}_k^H = \mathbf{h}_{d,k}^H + \mathbf{h}_{c,k}^H \boldsymbol{\theta} \mathbf{b}^H \in \mathbb{C}^{1 \times N_B}. \quad (2)$$

Stacking the user channels into the composite channel matrices $\mathbf{H}_d = [\mathbf{h}_{d,1}, \dots, \mathbf{h}_{d,K}]^H$ and $\mathbf{H}_c = [\mathbf{h}_{c,1}, \dots, \mathbf{h}_{c,K}]^H$, we obtain

$$\mathbf{H} = \mathbf{H}_d + \mathbf{H}_c \boldsymbol{\theta} \mathbf{b}^H \in \mathbb{C}^{K \times N_B} \quad (3)$$

where $\mathbf{H} = [\mathbf{h}_1, \dots, \mathbf{h}_K]^H$. Due to $\|\mathbf{b}\|_2 = 1$ and by defining

$$\mathbf{C} = \mathbf{H}_d \mathbf{P}_b^\perp \mathbf{H}_d^H, \quad \mathbf{D} = [\mathbf{H}_c, \mathbf{H}_d \mathbf{b}], \quad \bar{\boldsymbol{\theta}} = [\boldsymbol{\theta}^H \quad 1]^H \quad (4)$$

the Gram channel matrix can be written (similar to [8] and [9]) as

$$\mathbf{H}\mathbf{H}^H = \mathbf{C} + \mathbf{D}\bar{\boldsymbol{\theta}}\bar{\boldsymbol{\theta}}^H\mathbf{D}^H \in \mathbb{C}^{K \times K}. \quad (5)$$

III. DIRTY PAPER CODING

As performance metric, we consider the sum SE. In the high-SNR regime a scaled identity transmit covariance matrix in the dual uplink is optimal for DPC (see [15]). Together with (5) and $\bar{p} = P_{\text{Tx}}/K$, where P_{Tx} is the transmit power, the SE is given by

$$\begin{aligned} \text{SE}_{\text{DPC}} &= \log_2 \det(\mathbf{I} + \bar{p}\mathbf{H}\mathbf{H}^H) \\ &= \log_2 \det(\mathbf{I} + \mathbf{C}\bar{p}) + \log_2 \left(1 + \bar{\boldsymbol{\theta}}^H \mathbf{D}^H (\mathbf{I}/\bar{p} + \mathbf{C})^{-1} \mathbf{D}\bar{\boldsymbol{\theta}} \right). \end{aligned} \quad (6)$$

The asymptotic expression for $\bar{p} \rightarrow \infty$ is therefore

$$\overline{\text{SE}}_{\text{DPC}} = \log_2 \det(\mathbf{C}\bar{p}) + \log_2 \left(\bar{\boldsymbol{\theta}}^H \mathbf{D}^H \mathbf{C}^{-1} \mathbf{D}\bar{\boldsymbol{\theta}} \right) \quad (7)$$

in case \mathbf{C} is full rank. If $N_B = K$ one eigenvalue of \mathbf{C} is exactly zero (see next section) and we obtain the asymptotic expression ($\bar{p} \rightarrow \infty$)

$$\overline{\text{SE}}_{\text{DPC}} = \sum_{k=1}^{K-1} \log_2(\lambda_k \bar{p}) + \log_2 \left(\bar{p} |\mathbf{u}_K^H \mathbf{D}\bar{\boldsymbol{\theta}}|^2 \right) \quad (8)$$

where λ_k are the eigenvalues of \mathbf{C} in decreasing order and \mathbf{u}_k are the corresponding eigenvectors.

A. Optimal Phase Shift Solution

From (8), we can infer that if one eigenvalue of \mathbf{C} is zero, we can obtain the optimal solution of the phases by alignment as

$$\boldsymbol{\theta} = \exp \left(j \left(\angle(\mathbf{H}_c^H \mathbf{u}_K) - \angle(\mathbf{b}^H \mathbf{H}_d^H \mathbf{u}_K) \right) \right). \quad (9)$$

Quadratic System ($N_B = K$): The matrix \mathbf{C} has a zero eigenvalue if $\mathbf{b} \in \text{range}(\mathbf{H}_d^H)$. For specific scenarios, this is approximately fulfilled. However, in case $N_B = K$, one eigenvalue of \mathbf{C} is always exactly zero due to the orthogonal projector \mathbf{P}_b^\perp . For $\mathbf{b} \in \text{range}(\mathbf{H}_d^H)$, we have

$$\mathbf{u}_K = \frac{\mathbf{H}_d^{+,H} \mathbf{b}}{\|\mathbf{H}_d^{+,H} \mathbf{b}\|_2} \quad (10)$$

where for $N_B = K$ the pseudoinverse \mathbf{H}_d^+ is equal to \mathbf{H}_d^{-1} .

Rank Improvement Scenario: Additionally, the matrix \mathbf{C} also has a zero eigenvalue if \mathbf{H}_d has a zero singular value. This happens if the direct channels of some users are colinear or when we have a rank-improvement scenario where some users are blocked and, hence, have zero direct channel. For a rank-one BS-RIS channel only one of the blocked users is allocated (see [9], [8]) and we have

$$\mathbf{u}_K = \mathbf{e}_l \quad (11)$$

where l is the user with negligible direct channel. In this case, (9) is actually a channel gain maximization of user l (see [9]).

Optimal solution for high-SNR in case $K \geq N_B$: From the discussion above, we can directly give the optimal solution for a high-SNR scenario where we have more users than BS antennas. At high-SNR, N_B users will be allocated and the solution for the transmit covariance matrix is given by $\mathbf{I}\bar{p}$. According to above, the optimal phase shifts at the RIS are given by (9) with (10) as we have a quadratic system with $N_B = K$, due to the user allocation.

B. Phase Shift Heuristic

For $N_B = K$, the optimal phase shift vector is given by (9) with (10). In case $N_B > K$, we choose

$$\bar{\boldsymbol{\theta}}_{\text{opt}} = \exp(j(\angle(\mathbf{w}) - \mathbf{1}\angle(\mathbf{w}))). \quad (12)$$

where $\bar{\mathbf{w}}^T = [\mathbf{w}^T, w]$ is the eigenvector corresponding to the maximum eigenvalue of $\mathbf{D}^H(\mathbf{I}/\bar{p} + \mathbf{C})^{-1}\mathbf{D}$ to maximize SE_{DPC} in (6). To avoid the computation of an eigenvector in the dimension of the reflecting elements, we first compute the principal eigenvector $\bar{\mathbf{w}}' \in \mathbb{C}^K$ of the matrix $(\mathbf{I}/\bar{p} + \mathbf{C})^{-1}\mathbf{D}\mathbf{D}^H$ and then obtain the desired eigenvector (scaled version) $\bar{\mathbf{w}} = \mathbf{D}\bar{\mathbf{w}}'$. The complexity of the multiplication $\mathbf{D}\mathbf{D}^H$ is only linear in N_R . This also has to be calculated only once and for each user allocation (see Section IV-D) the specific submatrix can be deduced. It is important to note, that the above heuristic phase shift configuration is optimal in case one eigenvalue of \mathbf{C} is zero. The solution can be further refined with a local algorithm (e.g. element-wise) by using (12) as an initial guess.

IV. THOMLINSON HARASHIMA PRECODING

To avoid the implementation difficulties of DPC, we opt for vector perturbation precoding (see [12]). One suboptimal method is THP which avoids the computationally complex lattice search and can be employed with simple modulo transmitters/receivers. Specifically, the sent symbol in case of THP can be expressed as

$$\mathbf{x} = \mathbf{P}\mathbf{v} \in \mathbb{C}^{N_B} \quad (13)$$

with the transmit filter \mathbf{P} and the symbol

$$\mathbf{v} = \text{Mod}(\mathbf{s} + (\mathbf{I} - \mathbf{B})\mathbf{v}) \in \mathbb{C}^K \quad (14)$$

after the modulo chain, where $\mathbf{s} \in \mathbb{C}^K$ is the uniformly distributed data symbol and \mathbf{B} is the unit lower-triangular feedback filter. In particular, the real and imaginary part of the data symbol s_i is chosen to be uniformly distributed between -0.5 and 0.5. We use the popular reformulation (see, e.g., [16]) of the modulo operation which can be equivalently written by adding an integer vector \mathbf{a} resulting in $\mathbf{v} = \mathbf{s} + (\mathbf{I} - \mathbf{B})\mathbf{v} + \mathbf{a}$ and, hence, in the transmitted symbol

$$\mathbf{x} = \mathbf{P}\mathbf{B}^{-1}(\mathbf{s} + \mathbf{a}). \quad (15)$$

The receiver also employs a modulo operator and the signal

$$\begin{aligned} \mathbf{y} &= \text{Mod}(\mathbf{F}\mathbf{H}\mathbf{x} + \mathbf{F}\mathbf{n}) \\ &= \mathbf{F}\mathbf{H}\mathbf{x} + \mathbf{F}\mathbf{n} + \tilde{\mathbf{a}} \end{aligned} \quad (16)$$

is received. Here, $\mathbf{n} \sim \mathcal{N}_{\mathbb{C}}(\mathbf{0}, \mathbf{I})$, \mathbf{F} is the receive filter and $\tilde{\mathbf{a}}$ the integer vector corresponding to the modulo operator.

A. Zero-Forcing dTHP

Throughout this article, we consider zero-forcing THP (ZF-THP). Combining ZF-THP with a user allocation leads to good results also for moderate SNR values. There are two possibilities for ZF-THP (see, e.g., [17]): dTHP as well as cTHP. We observed that dTHP is particularly suited for a RIS-aided scenario and we will especially focus on this version within this article. A comment on cTHP is given in Section V. In this subsection, we give a short overview over THP, specifically, ZF-THP. For THP as well as other approaches like MMSE-THP see [16], [18], [10], [11]. Particularly, we select the transmit filters

$$\mathbf{B} = \text{diag}(\mathbf{l})^{-1}\mathbf{L}, \quad \mathbf{P} = \beta\mathbf{Q}^H \quad (17)$$

where \mathbf{L} and \mathbf{Q} are from the LQ-decomposition $\mathbf{H} = \mathbf{L}\mathbf{Q}$ and $\mathbf{l} = [L_{11}, \dots, L_{KK}]^T$. Because \mathbf{B} is unit lower-triangular,

$\frac{1}{L_{ii}} \sum_{j=1}^{i-1} L_{ij} v_j$ from $v_i = \text{Mod}(s_i - \frac{1}{L_{ii}} \sum_{j=1}^{i-1} L_{ij} v_j)$ only depends on s_j , $j < i$ and, hence, is independent of s_i . As, additionally, the real and imaginary parts of s_i are uniformly distributed between -0.5 and 0.5 , it follows that the real and imaginary parts of v_i are uniformly distributed between -0.5 and 0.5 as well. A proof for this well-known result is given in the Appendix. Hence, with the variance of a uniform distribution, we get

$$\mathbb{E}[|v_i|^2] = \frac{1}{6}. \quad (18)$$

Since \mathbf{Q} is unitary, the signal power of the sent symbol \mathbf{x} can be written as $\mathbb{E}[||\mathbf{x}||^2] = \beta^2 \frac{K}{6}$. Hence, we obtain the scaling $\beta = \sqrt{\frac{P_{\text{Tx}}}{K}}$ to match the power constraint $\mathbb{E}[||\mathbf{x}||^2] \leq P_{\text{Tx}}$ with equality. Choosing

$$\mathbf{F} = \text{diag}^{-1}(\mathbf{l}) \frac{1}{\beta} \quad (19)$$

as the receive filter, the received symbol is given by

$$\begin{aligned} \mathbf{y} &= \text{Mod}(\mathbf{F}\mathbf{H}\mathbf{P}\mathbf{B}^{-1}(\mathbf{s} + \mathbf{a}) + \mathbf{F}\mathbf{n}) \\ &= \text{Mod}\left(\mathbf{s} + \mathbf{a} + \frac{1}{\beta} \text{diag}^{-1}(\mathbf{l})\mathbf{n}\right) \end{aligned} \quad (20)$$

where \mathbf{a} vanishes due to the modulo operation. We arrive with K complex scalar modulo channels where for each of them, we can get for the SE (see, e.g., [19], [20], [21]) as

$$\text{SE}_k = -h \left(\text{Mod} \left(\sqrt{\frac{K}{P_{\text{Tx}} 6 L_{kk}^2}} \mathbf{n} \right) \right) \quad (21)$$

with the high-SNR asymptote (by using $\bar{p} = P_{\text{Tx}}/K$)

$$\bar{\text{SE}}_k = \log_2 \left(\frac{6}{\pi e} \bar{p} L_{kk}^2 \right). \quad (22)$$

Therefore, at high SNR the sum SE reads as

$$\bar{\text{SE}} = \log_2 \det(\bar{p}\mathbf{H}\mathbf{H}^H) - K \log_2 \left(\frac{\pi e}{6} \right) \quad (23)$$

since $\det(\mathbf{H}\mathbf{H}^H) = |\det \mathbf{L}|^2$. This is exactly the sum SE of DPC at high-SNR, however, we additionally have the shaping loss of approximately $K \log_2 \left(\frac{\pi e}{6} \right) \approx \frac{K}{2}$ bits for THP that is non-negligible.

B. Phase Shift Optimization

As the THP high-SNR sum SE is just the high-SNR DPC sum SE with an additional offset, the optimization of THP at high SNR can be directly transferred from Section III. The only difference is that $\mathbf{D}^H \mathbf{C}^{-1} \mathbf{D}$ [see (7)] is considered in comparison to $\mathbf{D}^H (\mathbf{I}/\bar{p} + \mathbf{C})^{-1} \mathbf{D}$ for $N_B > K$. In case one eigenvalue of \mathbf{C} is zero, e.g., when $N_B = K$, we arrive at (8).

C. Decoding Order

The high SNR sum SE only depends on the determinant of the Gram channel matrix and, hence, is independent of the decoding order. However, for lower SNR values this changes and we optimize the order based on the mean squared error (MSE). This metric was e.g. used in [16] and is more tractable than the SE in (21). Following [16], by defining $\hat{\mathbf{d}} = \mathbf{x} + \mathbf{a}$ at the transmitter and $\hat{\mathbf{d}} = \mathbf{y} - \mathbf{a}$ at the receiver, we can give the MSE as

$$\mathbb{E}[||\hat{\mathbf{d}} - \mathbf{d}||^2] = \mathbb{E}[||\mathbf{F}\mathbf{n}||^2] = \frac{K}{P_{\text{Tx}} 6} \sum_{k=1}^K \frac{1}{L_{kk}^2}. \quad (24)$$

To avoid a computationally complex search, the decoding order is determined by a successive approach. As in [16], we start with the user who is decoded lastly and then successively add users according

to the MSE criterion. It is important that we avoid a joint optimization of the phase shifts and the decoding order. Hence, for a certain user allocation, we first determine the high-SNR phase shift according to Section IV-B and then optimize the order for these phases.

D. User Allocation

In case, we have more users than BS antennas or if we only have medium SNR, it is not optimal to allocate all users for ZF-THP. Thus, we opt for a user allocation scheme. Specifically, we use a greedy scheme. This is often done in the literature for similar problems and has been applied for vector perturbation precoding in [20]. Accordingly, we start with the first user and successively add users one by one in a greedy manner as long as the sum SE increases. For the sum SE, we use the lower bound $\max(0, \bar{\text{SE}}_k)$ from (22) as a metric. Note that the phase shifts as well as the decoding order have to be optimized for each allocation. This complexity can be significantly reduced by exploiting the eigenvalue result in [8] as has been done in [22] for linear precoding. In this case, only two allocations have to be considered which clearly reduces the complexity. Additionally, one can follow [22] and use a two-norm relaxation for evaluating a user allocation by replacing $\bar{\boldsymbol{\theta}}^H \mathbf{D}^H \mathbf{C}^{-1} \mathbf{D} \bar{\boldsymbol{\theta}}$ with just $N_R \lambda_{\max}(\mathbf{D}^H \mathbf{C}^{-1} \mathbf{D}) = N_R \lambda_{\max}(\mathbf{C}^{-1} \mathbf{D} \mathbf{D}^H)$.

V. CENTRALIZED ZF-THP

We briefly comment on cTHP which is the alternative to dTHP (see, e.g., [17]). Here, the receive filter \mathbf{F} at the users is an identity matrix and, hence, the receivers just consist of a simple modulo receiver. While this reduces the receiver complexity, for cTHP, a joint optimization of the decoding order and the phases is important. Additionally, the high-SNR asymptote is not just the determinant and no simple solution is available as in case of dTHP and DPC. We also observed a significantly worse performance of cTHP and in summary it appears that it is not particularly suited for a RIS-aided scenario.

VI. DISCRETE PHASE SHIFTS

The simplicity of the objective for non-linear methods [see (7) and (8)] is especially beneficial for discrete phase shifts and we also evaluate the algorithms for a binary RIS, i.e., $\theta_n \in \{-1, 1\}$. The user allocation is still determined with continuous phase shifts. However, afterwards, the argument in the logarithm in (7) and (8) is then optimized by applying an element-wise algorithm where the continuous phase shift is chosen as an initial guess. Note that this initial guess is not feasible and only after the first iteration a valid discrete vector is obtained. Additionally, we extend the algorithm in [22] by replacing the element-wise algorithm based on continuous phase shifts by an element-wise algorithm on discrete phase shifts.

VII. SIMULATIONS

We consider an $N_B = 6$ antenna BS at (0, 0) m serving $K = 6$ single-antenna users which are uniformly distributed in a circle with radius 5 m at (75, 10) m. For all simulations, 3 of the users have an extra 60 dB pathloss of the direct channel. Hence, we simulate a rank-improvement scenario where at maximum 4 users will be served when including the RIS (see [9]). The position of the RIS is at (100, 0) m and the noise power is given by $\sigma^2 = -110$ dBm in all plots. We assume Rayleigh fading for the direct channels, Rician fading with a Rician factor of 0 dB for the channels between the RIS and the users and a pure LOS channel between the BS and the RIS. This pure LOS channel is defined by an outer product of two half-wavelength uniform linear array (ULA) vectors with both angles given by $\frac{\pi}{2}$. For Rayleigh/Rician fading, we assume the covariance matrices to follow a Laplacian angle density (see [23]) with an

angular standard deviation (ASD) of σ_{ASD} . Additionally, we choose the logarithmic pathloss model $L_{\text{dB}} = \alpha + \beta 10 \log_{10}(d)$ where d is the distance in meter. We consider three different sets of pathloss values for different channel strengths. Specifically, we use $L_{\text{dB,weak}} = 35.1 + 36.7 \log_{10}(d/m)$, $L_{\text{dB,strong}} = 37.51 + 22 \log_{10}(d/m)$, and $L_{\text{dB,LOS}} = 30 + 22 \log_{10}(d/m)$.

We are considering linear precoding as well as THP without the RIS (LISAwoRIS [24]/THPwoRIS), random phase shifts (LISARandom/THPRandom) as well as optimized versions with continuous (THP/AddOne-RIS-LISA) as well as discrete phase shifts (THP-Discrete/AddOne-RIS-LISA-Discrete). Furthermore, we use DPC-AO [25] as an upper bound with 10 initial phase shifts where the best is taken. Additionally, we include VP-Bound, which is the vector perturbation upper bound in [20], [21], [26] with the same user allocation and phase optimization method as in this article. Note that all THP results include the shaping loss [see (23)].

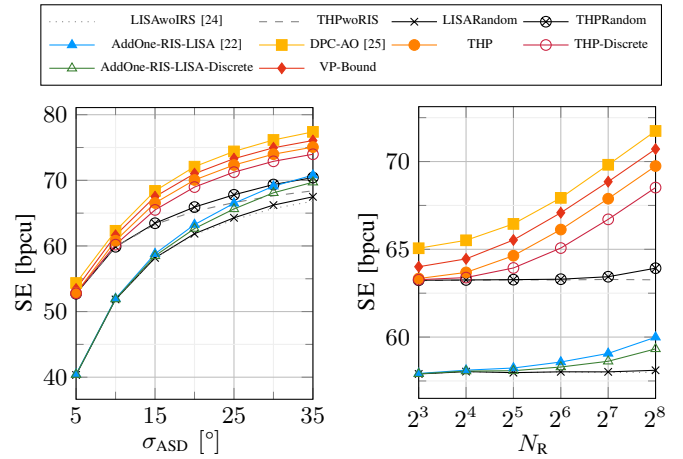
We first analyze the scenario w.r.t. the conditioning of the channel via the ASD. Here, we choose the direct, the RIS-user, as well as the BS-RIS channel to have an equally strong pathloss with $L_{\text{dB,strong}}$. In Fig. 1(a), we can see that THP is able to handle worse conditioning better than linear precoding. Specifically, we can see that THP allocates a new user (via the RIS) for a lower ASD in comparison to linear precoding. This has significant consequences as there are scenarios where the RIS has strong impact in case of THP but not for linear precoding. This is further investigated in Fig. 1(b) based on $\sigma_{\text{ASD}} = 15^\circ$. Here, linear precoding has severe problems in the sense that even for a higher number of elements no or only a very slight increase in the SE is possible. In comparison, the SE of THP is significantly increased, also for a smaller number of elements.

We choose now a scenario where the channels are better conditioned $\sigma_{\text{ASD}} = 30^\circ$ and the RIS has more impact, which is beneficial for the linear methods. Specifically, the users are assumed to be closer to the RIS by shifting the circle from (75, 10)m to (95, 10)m. Additionally, we assume $L_{\text{dB,weak}}$ for the direct channels and $L_{\text{dB,LOS}}$ for the BS-RIS channel. From Fig. 2(a) we can infer that the linear methods achieve now also a good performance. However, a higher number of reflecting elements is needed, which is especially pronounced for discrete phase shifts.

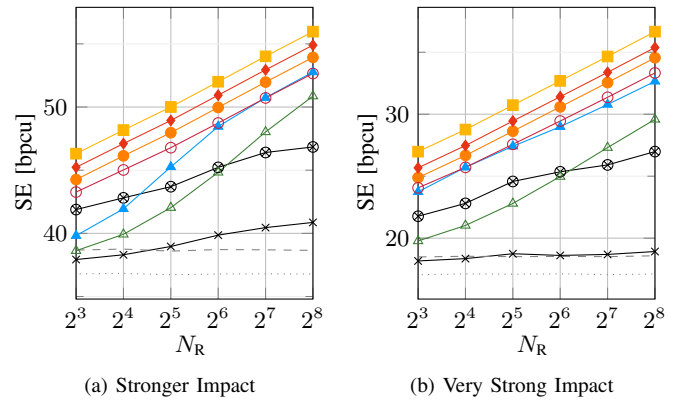
In Fig. 2(b) we set an additional pathloss of 20 dB for the 3 stronger users and, hence, the RIS has an even stronger impact. Here, we can see the fundamental limits for random and statistical phase shifts according to [9] and linear precoding with random phase shifts is severely limited in comparison to THP with random phase shifts. For instantaneous phase shifts on the other hand, the linear methods result in a comparable performance, even though THP still leads to better results. The discrete phases in case of linear precoding are still limited and there exists a major gap to the THP methods.

VIII. CONCLUSION

Similar to DPC, THP, taking into account the shaping loss, leads to fundamental advantages in comparison to linear precoding in a RIS assisted scenario. Especially, when the BS-RIS channel is not orthogonal to the direct channel or for random/statistical phase shifts, THP has its advantages which are even more pronounced for discrete phases. Future work will consider non-ZF THP, vector perturbation precoding and the important case of statistical phase shifts.



(a) Orthogonality, $N_R = 64$ (b) RIS Elements, $\sigma_{\text{ASD}} = 15^\circ$
Fig. 1. SE for lower impact of the RIS



(a) Stronger Impact (b) Very Strong Impact
Fig. 2. SE for strong impact of the RIS with $\sigma_{\text{ASD}} = 30^\circ$

APPENDIX

For two independent random variables X and N where $X \sim \mathcal{U}(-0.5, 0.5)$, the distribution $Y = \text{Mod}(X + N)$ is again uniformly distributed between -0.5 and 0.5 . To see this, we first give the distribution for $W = X + N$ which is

$$f_W(w) = \int_{-\infty}^{\infty} f_N(\tau) f_X(w - \tau) d\tau. \quad (25)$$

As $f_X(x) = 1$ for $-0.5 \leq x \leq 0.5$ we have

$$f_W(w) = \int_{w-0.5}^{w+0.5} f_N(\tau) d\tau. \quad (26)$$

The distribution of $Y = \text{Mod}(X + N) = \text{Mod}(W)$ is given by

$$f_Y(y) = \begin{cases} \sum_{k \in \mathbb{Z}} f_W(y + k) & -0.5 \leq y \leq 0.5 \\ 0 & \text{else.} \end{cases} \quad (27)$$

And as, additionally,

$$\begin{aligned} \sum_{k \in \mathbb{Z}} f_W(y + k) &= \sum_{k \in \mathbb{Z}} \int_{w+k-0.5}^{w+k+0.5} f_N(\tau) d\tau \\ &= \int_{-\infty}^{\infty} f_N(\tau) d\tau = 1 \end{aligned} \quad (28)$$

holds, we have $Y \sim \mathcal{U}(-0.5, 0.5)$.

REFERENCES

- [1] Q. Wu and R. Zhang, "Intelligent Reflecting Surface Enhanced Wireless Network via Joint Active and Passive Beamforming," *IEEE Transactions on Wireless Communications*, vol. 18, no. 11, pp. 5394–5409, 2019.
- [2] H. Guo, Y.-C. Liang, J. Chen, and E. G. Larsson, "Weighted Sum-Rate Maximization for Reconfigurable Intelligent Surface Aided Wireless Networks," *IEEE Transactions on Wireless Communications*, vol. 19, no. 5, pp. 3064–3076, 2020.
- [3] C. Pan, H. Ren, K. Wang, W. Xu, M. ElKashlan, A. Nallanathan, and L. Hanzo, "Multicell MIMO Communications Relying on Intelligent Reflecting Surfaces," *IEEE Transactions on Wireless Communications*, vol. 19, no. 8, pp. 5218–5233, 2020.
- [4] S. Zhang and R. Zhang, "Capacity Characterization for Intelligent Reflecting Surface Aided MIMO Communication," *IEEE Journal on Selected Areas in Communications*, vol. 38, no. 8, pp. 1823–1838, 2020.
- [5] Q. Wu and R. Zhang, "Towards Smart and Reconfigurable Environment: Intelligent Reflecting Surface Aided Wireless Network," *IEEE Communications Magazine*, vol. 58, no. 1, pp. 106–112, 2020.
- [6] Q.-U.-A. Nadeem, A. Kammoun, A. Chaaban, M. Debbah, and M.-S. Alouini, "Asymptotic Max-Min SINR Analysis of Reconfigurable Intelligent Surface Assisted MISO Systems," *IEEE Transactions on Wireless Communications*, vol. 19, no. 12, pp. 7748–7764, 2020.
- [7] A. Papazafeiropoulos, P. Kourtessis, K. Ntontin, and S. Chatzinotas, "Joint Spatial Division and Multiplexing for FDD in Intelligent Reflecting Surface-Assisted Massive MIMO Systems," *IEEE Transactions on Vehicular Technology*, vol. 71, no. 10, pp. 10754–10769, 2022.
- [8] D. Semmler, M. Joham, and W. Utschick, "High SNR Analysis of RIS-Aided MIMO Broadcast Channels," in *2023 IEEE 24th International Workshop on Signal Processing Advances in Wireless Communications (SPAWC)*, 2023, pp. 221–225.
- [9] D. Semmler, B. Fesl, M. Joham, and W. Utschick, "High-SNR Comparison of Linear Precoding and DPC in RIS-Aided MIMO Broadcast Channels," *arXiv*, <https://arxiv.org/abs/2405.18859>, 2024. [Online]. Available: <https://arxiv.org/abs/2405.18859>
- [10] M. Tomlinson, "New automatic equaliser employing modulo arithmetic," *Electronics Letters*, vol. 7, pp. 138–139(1), March 1971.
- [11] H. Harashima and H. Miyakawa, "Matched-Transmission Technique for Channels With Intersymbol Interference," *IEEE Transactions on Communications*, vol. 20, no. 4, pp. 774–780, 1972.
- [12] B. Hochwald, C. Peel, and A. Swindlehurst, "A vector-perturbation technique for near-capacity multiantenna multiuser communication-part ii: perturbation," *IEEE Transactions on Communications*, vol. 53, no. 3, pp. 537–544, 2005.
- [13] J. A. Nossek, D. Semmler, M. Joham, and W. Utschick, "Physically Consistent Modeling of Wireless Links With Reconfigurable Intelligent Surfaces Using Multipoint Network Analysis," *IEEE Wireless Communications Letters*, vol. 13, no. 8, pp. 2240–2244, 2024.
- [14] D. Semmler, J. A. Nossek, M. Joham, and W. Utschick, "Performance Analysis of Systems with Coupled and Decoupled RISs," in *2024 19th International Symposium on Wireless Communication Systems (ISWCS)*, 2024, pp. 1–6.
- [15] J. Lee and N. Jindal, "High SNR Analysis for MIMO Broadcast Channels: Dirty Paper Coding Versus Linear Precoding," *IEEE Transactions on Information Theory*, vol. 53, no. 12, pp. 4787–4792, 2007.
- [16] M. Joham, D. A. Schmidt, J. Brehmer, and W. Utschick, "Finite-Length MMSE Tomlinson–Harashima Precoding for Frequency Selective Vector Channels," *IEEE Transactions on Signal Processing*, vol. 55, no. 6, pp. 3073–3088, 2007.
- [17] K. Zu, R. C. de Lamare, and M. Haardt, "Multi-Branch Tomlinson-Harashima Precoding Design for MU-MIMO Systems: Theory and Algorithms," *IEEE Transactions on Communications*, vol. 62, no. 3, pp. 939–951, 2014.
- [18] C. Windpassinger, R. Fischer, T. Vencel, and J. Huber, "Precoding in multiantenna and multiuser communications," *IEEE Transactions on Wireless Communications*, vol. 3, no. 4, pp. 1305–1316, 2004.
- [19] G. Forney, M. Trott, and S.-Y. Chung, "Sphere-bound-achieving coset codes and multilevel coset codes," *IEEE Transactions on Information Theory*, vol. 46, no. 3, pp. 820–850, 2000.
- [20] A. Razi, D. J. Ryan, I. B. Collings, and J. Yuan, "Sum Rates and User Scheduling for Multi-User MIMO Vector Perturbation Precoding," in *2009 IEEE International Conference on Communications*, 2009, pp. 1–5.
- [21] M. Barrenechea, M. Joham, M. Mendicute, and W. Utschick, "Analysis of Vector Precoding at High SNR: Rate Bounds and Ergodic Results," in *2010 IEEE Global Telecommunications Conference GLOBECOM 2010*, 2010, pp. 1–5.
- [22] D. Semmler, M. Joham, and W. Utschick, "A Zero-Forcing Approach for the RIS-Aided MIMO Broadcast Channel," in *ICC 2024 - IEEE International Conference on Communications*, 2024, pp. 4378–4383.
- [23] Z. Jiang, A. F. Molisch, G. Caire, and Z. Niu, "Achievable Rates of FDD Massive MIMO Systems with Spatial Channel Correlation," *IEEE Transactions on Wireless Communications*, vol. 14, no. 5, pp. 2868–2882, 2015.
- [24] C. Guthy, W. Utschick, R. Hunger, and M. Joham, "Efficient Weighted Sum Rate Maximization With Linear Precoding," *IEEE Transactions on Signal Processing*, vol. 58, no. 4, pp. 2284–2297, 2010.
- [25] N. S. Perović, L.-N. Tran, M. D. Renzo, and M. F. Flanagan, "On the Maximum Achievable Sum-Rate of the RIS-Aided MIMO Broadcast Channel," *IEEE Transactions on Signal Processing*, vol. 70, pp. 6316–6331, 2022.
- [26] D. J. Ryan, I. B. Collings, I. V. L. Clarkson, and R. W. Heath Jr., "A Lattice-Theoretic Analysis of Vector Perturbation for Multi-User MIMO Systems," in *2008 IEEE International Conference on Communications*, 2008, pp. 3340–3344.